# Simulating Scanning Tunneling Microscope Measurements

by

Vivek Venkatachalam

Submitted to the Department of Physics in partial fulfillment of the Requirements for the Degree
BACHELOR OF SCIENCE
at the
MASSACHUSETTS INSTITUTE OF TECHNOLOGY
June, 2006









Signature of Author
Department of Physics
May 12, 2006

Certified by
Professor Eric W. Hudson
Thesis Supervisor, Department of Physics

Accepted by
Professor David E. Pritchard
Senior Thesis Coordinator, Department of Physics

# Table of Contents

# Introduction

One of the largest problems in scanning tunneling microscopy design is noise control. It is the burden of the designer to determine if money should be used to build a floating room for vibration isolation or for top-of-the-line preamplifiers that can be placed at low temperatures. This thesis presents a simulation of the STM measurement chain, from tunneling tip to computer control. The goal is to see how noise at different stages of the measurement chain affect the output of spectroscopy (density of states) measurements.

Specifically, we look at how spectroscopy measurements depend on the temperature of the sample, the density of states in the sample and tip, the shakiness of the tip, the noise present in the current preamplifier, and several other settings. Chapter 1 describes STM spectroscopy measurement, Chapter 2 explains how it is simulated, and Chapter 3 finally looks at the results of various simulations.

# Chapter 1

# Overview of Scanning Tunneling Microscopy

The 1986 Nobel Prize in physics was given to Binnig and Rohrer for developing the scanning tunneling microscope. [2] The microscope requires application of a voltage between an atomically sharp tip and atomically flat surface separated by a vacuum barrier. One of the simplest predictions of quantum theory is that electrons can tunnel through this classically forbidden vacuum between sample and tip, producing a tunneling current which sensitively depends on the tip-sample separation as well as electronic properties of the sample. A schematic of STM operation is given in Figure 1.1.

## 1.1 The Tunneling Current

### 1.1.1 Barrier Dependence of Current

The sensitivity of the tunneling current to tip-sample separation can easily be determined using the WKB approximation for a square barrier. Namely, the tunneling probability (amplitude squared) is given by

$$|M|^2 = \exp\left(-2\int_0^s dx\sqrt{\frac{2m\varphi}{\hbar^2}}\right) = e^{-\frac{2s}{s_0}}, \tag{1.1}$$

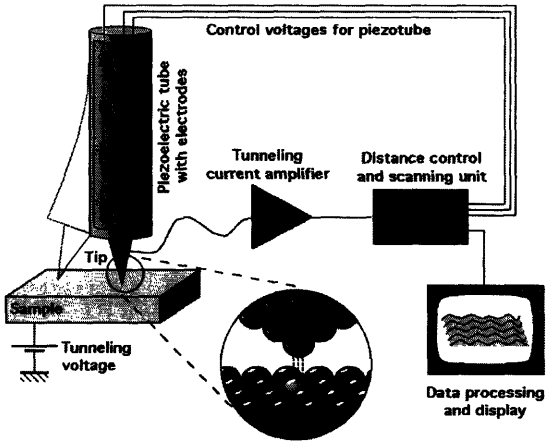


Figure 1.1: The STM operates by applying a bias voltage between tip and sample, and measuring the resulting current that tunnels between the tip and sample. This current depends on both separation and electronic properties of the sample.

where $s_0 = \sqrt{\frac{\hbar^2}{2m\varphi}}$. The potential height, $\varphi$, is determined by the work functions of the sample and tip, so greater work functions correspond to greater sensitivity of the tip current to variations in height. Typical values for $\varphi$ are on the order of a few eVs [3], giving a characteristic decay length of $s_0 \approx 1$Å.

If we use feedback to maintain a constant tunneling current through the tip while sweeping across a sample, we will necessarily be maintaining a constant tunneling barrier. Thus, by plotting the height of the tip as a function of position, we can obtain information about the topography of a sample. Given adequate vibration isolation, this topography can have atomic resolution.

### 1.1.2 Electronic Dependence of Current

Even with small tip-sample separation, tunneling will only occur if there are occupied states to tunnel from and unoccupied states to tunnel into. Fermi's golden rule gives the current due to elastic tunneling from the tip to the sample at energy $\epsilon$ as

$$dI_{st}(\epsilon) = \frac{2\pi}{\hbar}(-2e|M|^2)[\rho_s(\epsilon)f(\epsilon)][\rho_t(\epsilon + eV)(1 - f(\epsilon + eV))]. \qquad (1.2)$$

The factor of $-2e$ prefixing the matrix element accounts for spin degeneracy and sign of the electron charge. The expression $\rho_s(\epsilon)f(\epsilon)$ gives the number of states available for tunneling from (density of sample energy states at energy $\epsilon$ smeared by the fermi function due to nonzero temperature), and $\rho_t(\epsilon+eV)(1-f(\epsilon+eV))$ gives the number of states available for tunneling into. It is also possible for electrons to tunnel from the tip to the sample, with current

$$dI_{ts}(\epsilon) = \frac{2\pi}{\hbar}(-2e|M|^2)[\rho_t(\epsilon+eV)f(\epsilon+eV)][\rho_s(\epsilon)(1-f(\epsilon))]. \tag{1.3}$$

Total current is obtained by combining the tip→sample and sample→tip contribu-

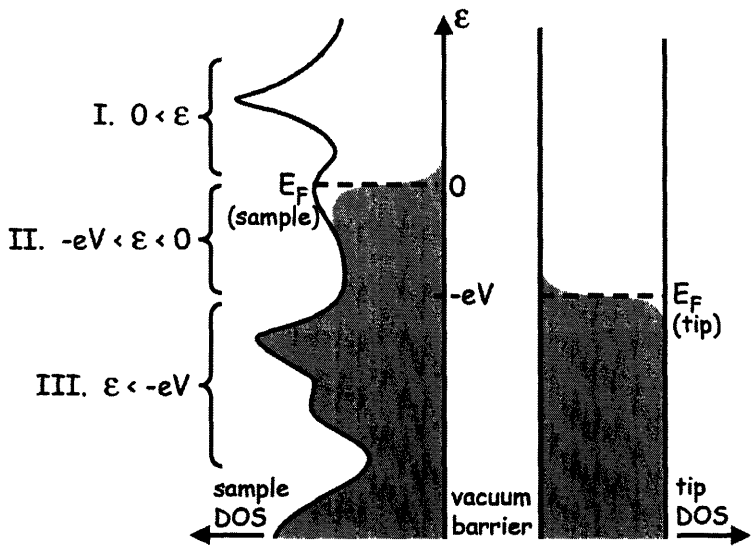


Figure 1.2: With a negative bias voltage $V$ applied to the sample, its electrons will be at a higher potential than those in the tip. The tunneling probability from sample to tip is determined by separation as well as how many states are available to tunnel into or out of. Figure from [3].

tions and integrating over all energies:

$$I = \frac{4\pi e}{\hbar}e^{-2s/s_0}\int_0^\infty d\epsilon\rho_s(\epsilon)\rho_t(\epsilon+eV)\ (f(\epsilon)[1-f(\epsilon+eV)] - [1-f(\epsilon)]f(\epsilon+eV)) \tag{1.4}$$

If we assume that we are working at very low temperatures ($kT \ll eV$), the fermi function can be approximated with a step function. It is clear that in this limit, the only contribution to tunneling will be from energies $\epsilon$ between $-eV$ and 0. With these approximations, the expression for tunneling current is now

$$I \approx \frac{4\pi e}{\hbar} e^{-2s/s_0} \int_{-eV}^{0} d\epsilon \rho_s(\epsilon)\rho_t(\epsilon + eV). \tag{1.5}$$

If we choose a tip with constant density of states in the desired region (here $\epsilon = E_f$ to $\epsilon = E_f + eV$), we get the simpler expression

$$I \approx \frac{-4\pi e}{\hbar} e^{-2s/s_0} \rho_t(0) \int_{-eV}^{0} d\epsilon \rho_s(\epsilon). \tag{1.6}$$

Our current is now related to the integrated density of states in the sample. To obtain the more interesting quantity $\rho_s(\epsilon)$, we simply need to differentiate the expression for $I$

$$\frac{dI}{dV} \approx \frac{4\pi e^2}{\hbar} e^{-2s/s_0} \rho_t(0)\rho_s(eV). \tag{1.7}$$

Thus, by measuring the differential conductance $\frac{dI}{dV}$ at low temperatures, we can gain very direct information about both the sample-tip separation, $s$, and the local density of states $\rho_s(eV)$.

## 1.2 Noise

The largest obstacle to obtaining high-quality data from the STM is the presence of environmental noise, both mechanical and electrical.

### 1.2.1 Vibration Isolation

All of the previously described measurements rely on the ability to maintain a constant separation between tip and sample. If the tip-sample separation separation suffers from noise of even a few angstroms, we would not be able to obtain meaningful information from the tunneling current. Also, vibrations can move wires around, which couple capacitively to other electronic components and generate noise.

Our experimental setup floats on a 4000 pound granite block resting on air springs. Cables are tied down wherever possible to prevent microphonic pickup. To further isolate the microscope from mechanical noise, we have put in a damped-spring system at the bottom of the fridge(see Figure 1.3).

### 1.2.2 Electronic Noise

The small tunneling current that emerges from the microscope must be amplified to measurable levels. If mechanical noise has been properly handled, the noise introduced during (and before) this amplification limits the ability of our microscope. The three dominant forms of electronic noise in the system are Johnson noise, 1/f noise, and shot noise.

The Johnson noise across a resistor is given by $\Delta V = \sqrt{4kTR\,\Delta f}$. Though the noise increases with resistance ($\propto R^{1/2}$), it should be noted that the voltage grows linearly ($V = IR$), so large values of $R$ still give better signal to noise ratios. Our preamplifier provides a gain of $10^{-9}$ A/V, suggesting a resistance of about 1 G$\Omega$. For a preamplifier operating at room temperature, this corresponds to noise of $\Delta V = 4.07\mu V/\sqrt{\text{Hz}}$.

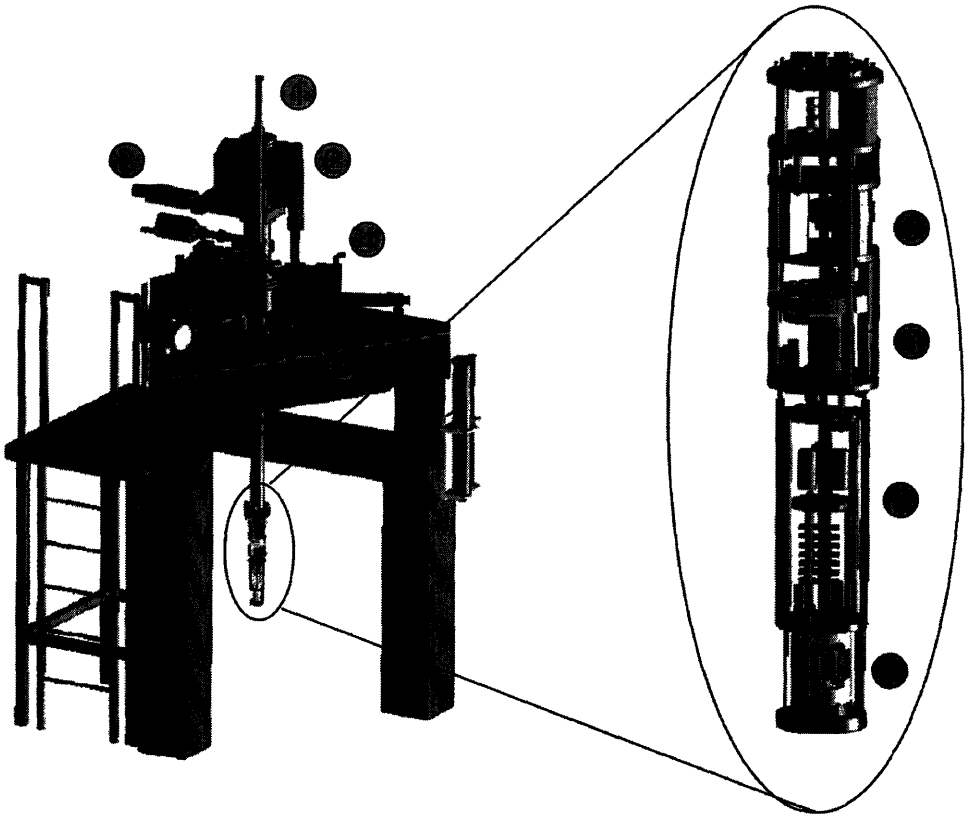

Figure 1.3: CAD drawings of our experimental setup. The blowup on the right is the fridge which houses the STM. (1) Rods to move our sample towards the microscope and manipulate various components of the fridge. (2) Ion pump to maintain low pressure in our chambers. (4) Turbo pump, which is used to bring the pressure to UHV levels ($10^{-11}$ torr). When the experiment is running, the turbo pump is turned off due to its high vibration levels. (5) Granite table resting on air springs for vibration isolation. (6) Rotary stage where samples can be stored. (7) Cleaver to make surfaces atomically flat, as is required for STM studies. (8) In vacuum isolation to further reduce noise, consisting of springs and an eddy-current damping mechanism. (9) The microscope itself.

# Chapter 2

# Modelling the STM Measurement Process

This chapter will provide an overview of the various components involved in the STM measurement chain and how they were modelled using MATLAB and Simulink® to simulate spectroscopic (LDOS) measurements with our microscope.

## 2.1 The Microscope

As we mentioned in the previous chapter, the current across the tip is given by Equation 1.4:

$$I = \frac{4\pi e}{\hbar} e^{-2s/s_0} \int_0^\infty d\epsilon \rho_s(\epsilon)\rho_t(\epsilon + eV)\ (f(\epsilon)[1 - f(\epsilon + eV)] - [1 - f(\epsilon)]f(\epsilon + eV)) \tag{2.1}$$

Each density of states ($\rho_s$ and $\rho_t$) is represented by a 2101 component vector providing the DOS values in arbitrary units from -105 meV to 105 meV (resolution of 0.1 meV) (See Figure 2.1). Our eventual goal is to measure the differential conductance ($\frac{dI}{dV}$), which is related to the density of states in the sample. It may seem that we should simply increase the voltage across the sample to obtain $I(V)$ and then differentiate that to obtain the desired quantity. In practice, however, it much cleaner to do the differentiation using electronics (e.g. a lock-in amplifier).

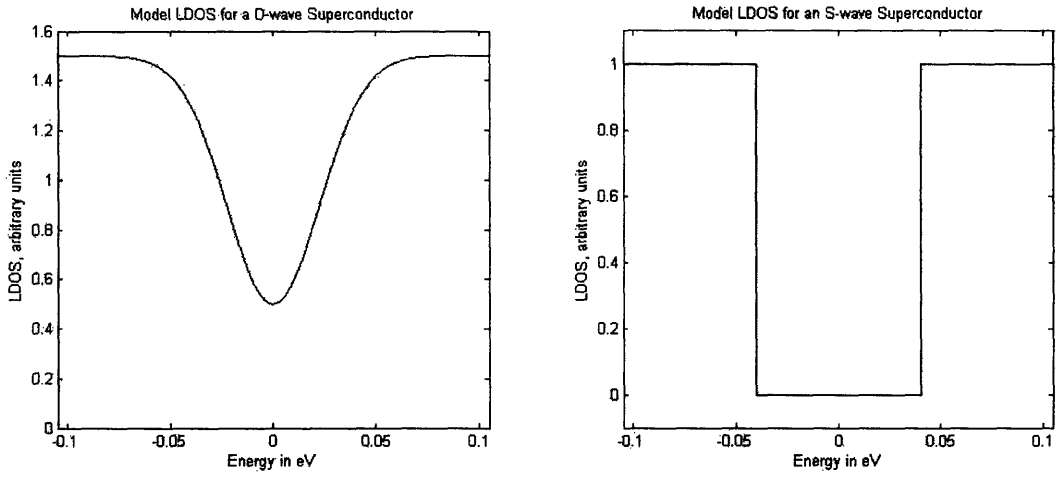


Figure 2.1: Sample local density of state (LDOS) profiles that can be used in simulations. Traditional superconductors fall into the s-wave category and have rectangular gaps at the fermi energy. Unconventional (Type II) superconductors can have triangular (d-wave) energy gaps at their fermi surface. Most of the simulations in this paper were conducted using a flat density of states for the tip and an inverted Gaussian (d-wave like) density of states for the sample.

If we send in a signal $V_0 + \epsilon \sin(\omega_r t)$, the output will be

$$I = I(V_0) + \left[\frac{dI}{dV}\right]_{V=V_0} \epsilon \sin(\omega_r t) + \mathcal{O}(\epsilon^2) \tag{2.2}$$

. By measuring the AC component of this output (and dividing by $\epsilon$), we can find the differential conductance without resorting to the less reliable practice of numerical differentiation.

To obtain a resolution of 1 meV in LDOS, we will use that as our step size for the DC component of the voltage applied to the sample. On top of this DC step will be an AC signal. At each time step, we take the voltage applied to the sample (along with $\rho_s, \rho_t$, and the temperature $T$) and use equation 2.1 to determine the total tunneling current.

The output current is normalized to have an rms value of 1 (in practice, active feedback is used to maintain the value of the rms current). This current is then sent on to the next segment of the simulation, the preamplifier.

### 2.1.1 Tip Noise

There are two ways in which movement of the tip can introduce noise into STM measurements. Horizontal movement of the tip can change the area of the sample where the tip is located, thereby changing the energy spectrum being observed. To mimic this, we could add the appropriate noise to the LDOS vector used for $\rho_s$ or $\rho_t$. While there is room in the simulation to add this noise, it has not been used in the simulations presented in this thesis.

A more noticeable way in which the tip's height affects noise is through vertical motion. The tunneling current depends exponentially on the tip's height, so small noise in $s$ (see Equation 1.1) can have a dramatic effect on the measured current. By considering white noise (flat power spectrum up to 10 kHz, the sample frequency) of various amplitudes on the tip, we can gauge the amount of tip noise the measurement process can tolerate. This, in return, can give us information about the amount of vibration isolation required to stabilize the tip. More details on results from varying

$s$ noise are given in Chapter 3.

A diagram of the tip simulation is given in Figure 2.2.

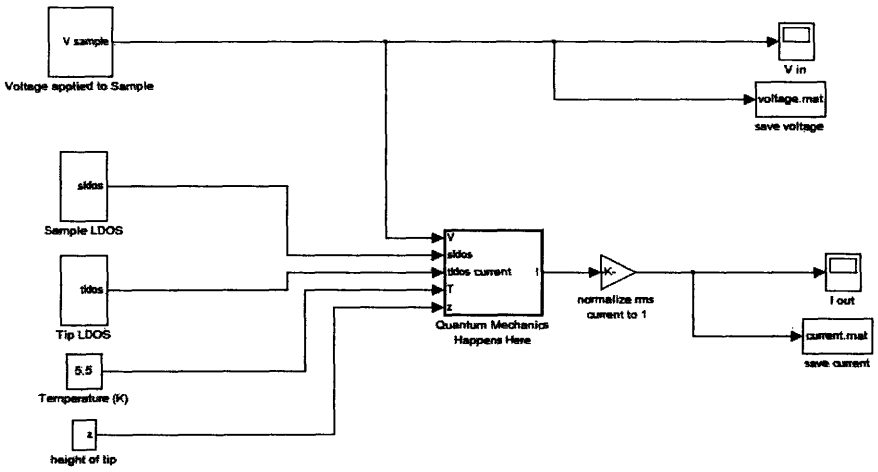


Figure 2.2: A diagram of the simulation used to model the physics taking place in the microscope proper.

## 2.2 Electronics

While the voltage to current process described above accounts for nearly all of the interesting physics involved in STM measurements, more electronic work is needed to convert the resulting tunneling current into a measurable signal. A current preamplifier is used to provide the initial amplification to the signal, a lock-in amplifier is used to isolate the frequency of interest, and an experimental computer is finally used to average the resulting signal and convert it to a simple plot of differential conductance versus energy for the sample.

### 2.2.1 The Preamplifier

We utilized a DL Instruments Model 1211 preamplifier for current amplification. A schematic is given in Figure 2.3.

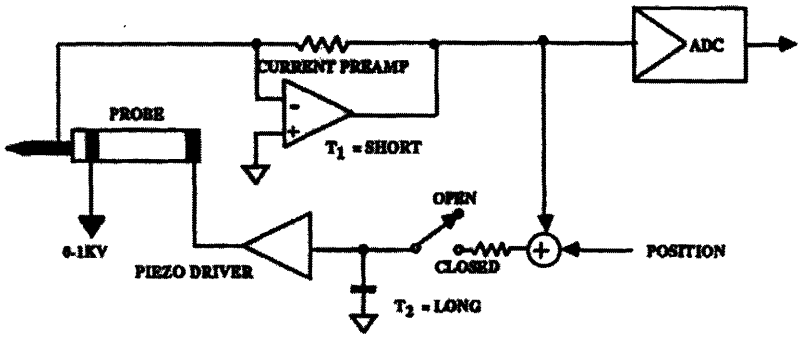


Figure 2.3: A schematic of how the preamplifier is connected in the STM measurement chain. Figure from [4].

The preamplifier essentially consists of an operational amplifier in feedback mode to hold the negative terminal at virtual ground. The current flowing through the feedback resistor determines the output voltage of the op-amp ($V = IR$). The setting we use for our measurements is a gain of $10^9$ V/A, or a resistance of about 1 G$\Omega$. For our settings, the published noise level is 4.26 $\mu V/\sqrt{\text{Hz}}$, very close to the 4.07 $\mu V/\sqrt{\text{Hz}}$ minimum calculated earlier. [4]

Also present in the DL 1211 preamplifier is an output filter. For a risetime setting of about 300 $\mu$s and a 12 dB/octave rolloff, this is given by a 2-pole lowpass filter with a 6 dB corner frequency of 1780 Hz (see Table 2 in [4]). Namely,

$$H_{preamp}(s) = \frac{1}{\left(1 + \frac{s}{2\pi(1780\text{Hz})}\right)^2} \tag{2.3}$$

Also from [4], we find that the equivalent noise bandwidth for this setting is 1400 Hz.

A schematic of the preamplifier simulation is given at the top of Figure 2.4.

### 2.2.2 The Lock-In Amplifier

The signal from the preamplifier is sent to a lock-in amplifier which is responsible for extracting the AC signal which carries information about the differential conductance of the sample. We use an SRS Model SR830 DSP lock-in amplifier for all

of our measurements.

The lock-in first multiplies the incoming signal by a pure sine wave that is matched (or "locked in") to the frequency of the signal driving the experiment ($\omega_r$ in Equation 2.2). The resulting signal will have components at both $\omega_r + \omega_L$ and $\omega_r - \omega_L$, where $\omega_L$ is the lock-in frequency. If $\omega_r$ is well-matched to $\omega_L$, the difference signal will be DC. After narrow-band low-pass filtering, this DC signal proportional to the original AC signal will be all that remains. Thus the DC output of the lock-in is thus proportional to $dI/dV$ as desired.

For a single channel lock-in, problems can arise if the phase of the input signal and the reference signal are off by $\pi/2$. However, the SR830 uses a dual-channel mode to get both the in-phase ($\sin(\omega_r t)$) and out-of-phase ($\cos(\omega_r t)$) components of the input signal. These two components are added in quadrature to get the final $dI/dV$ signal. A schematic of the lock-in is given in Figure 2.4.

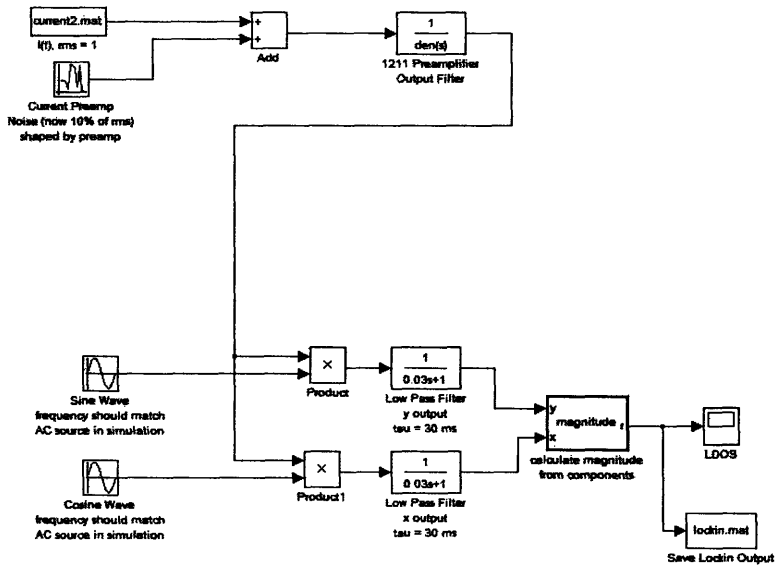


Figure 2.4: A diagram showing the simulation of the preamplifier (top) and the lock-in amplifier (bottom)

### 2.2.3 The Experimental Control Unit

The experimental control unit (ECU) is responsible for sending the voltage signal to the microscope and interpreting the voltage that is returned (should be $dI/dV$). By averaging over the signal that comes out of the lock-in and comparing it to the voltage signal being sent to the sample, the ECU can create a plot of differential conductance (related to LDOS) versus energy. This is our final goal in spectroscopy measurements. The averaging done by the ECU is handled by a simple MATLAB script instead of the Simulink software used for the other parts of the simulation.

# Chapter 3

# Simulation Results

This chapter contains the results of various simulations using the program described in Chapter 2.

## 3.1 Default Parameters

The default parameters used in these simulations are provided in Table 3.1. They correspond to the plot in Figure 3.1. Each section essentially corresponds to one of these parameters being varied.

| Parameter | Value |
|---|---|
| Temperature | 5 K |
| Tip Height Noise | 1% |
| Preamp Noise | 10% of rms input current |
| DC Bias Step size | 1 meV |
| AC Bias Amplitude | 2.5 meV |
| ECU Averaging Time | 150 ms |
| $\rho_t$ | constant |
| $\rho_s$ | triangular gap (see Figure 2.1) |

## 3.2 Varying Temperature

Temperature determines which energetic states are occupied. At zero temperature, fermions occupy all states from the ground state to the Fermi energy in accordance

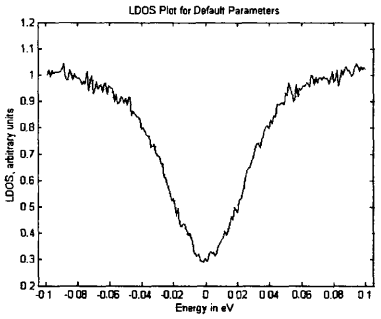


Figure 3.1: Plot generated using default parameters.

with the Pauli exclusion principle. At nonzero temperature, some of the high energy fermions are excited to states above the Fermi surface. For conventional metals these excitations can have arbitrarily low energy while in superconductors they are gapped (with the gap size corresponding to the energy needed to break a Cooper Pair).

In either case, to determine the actual energetic distribution of electrons in a either the tip or sample, we simply have to multiply the density of states ($\rho_s$ or $\rho_t$) by the Fermi funtion:

$$f(\epsilon) = \frac{1}{1 + e^{\epsilon/kT}} \tag{3.1}$$

In the zero temperature limit, we showed that the differential conductance is proportional to the density of states at the given bias energy. At small temperatures, this begins to break down. At sufficiently high temperatures, the differential conductance is no longer a simple indicator of the LDOS in the sample.

Figure 3.2 shows the effect of increasing temperature on the model density of states shown in the left panel of Figure 2.1. As we increase the temperature, we see that the gap gets shallower and shallower, eventually disappearing at room temperature.

In general, our resolution for spectroscopy is given by $k_B T$. At 5 K, we can resolve DOS features as small as 0.43 meV. At room temperature, however, we can only resolve down to 26 meV. The primary DOS features of interest are energy gaps,

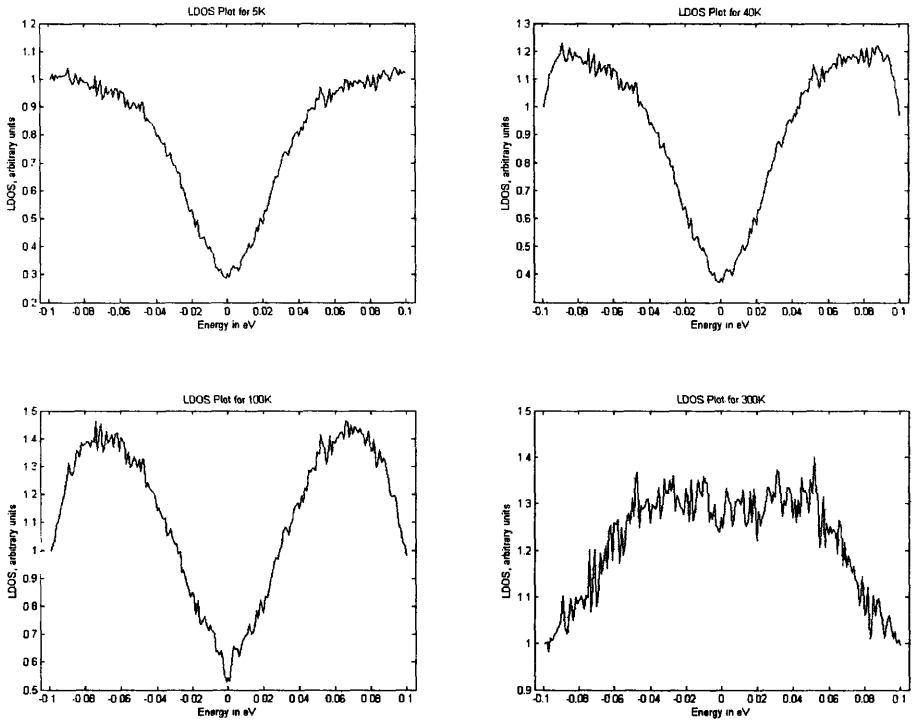


Figure 3.2: Plots of the observed density of states inferred from differential conductance. As expected, increasing the temperature has the effect of smearing out (averaging) features in the original DOS curve. The dips at the edges of the plots are artifacts of limiting the range of energies integrated over to calculate the tunneling current.

generally 10s of meV, which can be well resolved nearly up to room temperature. Also of interest are DOS "spikes" that generally appear around the energy gap when a sample is in the superconducting phase. These spikes are generally only a few eVs and cannot be well-resolved as temperatures increase over 50 K. This can cause problems when trying to identify the superconductor to pseudogap phase transition temperature ($T_c$) in high-temperature superconductors.

It should be noted here that all of the interesting physics associated with temperature changes occur in the sample (phase transitions, etc.), and result in the density of states changing, not just being smeared by the fermi function. None of this is captured in these simulations, which focus on the STM measurement chain.

## 3.3 Superconducting Tip

If we use a superconducting tip, the differential conductance certainly doesn't correspond to the density of states in the simple way described in Chapter 1. Plots of what we might expect if both tip and sample have triangular energy gaps are given in Figure 3.3.

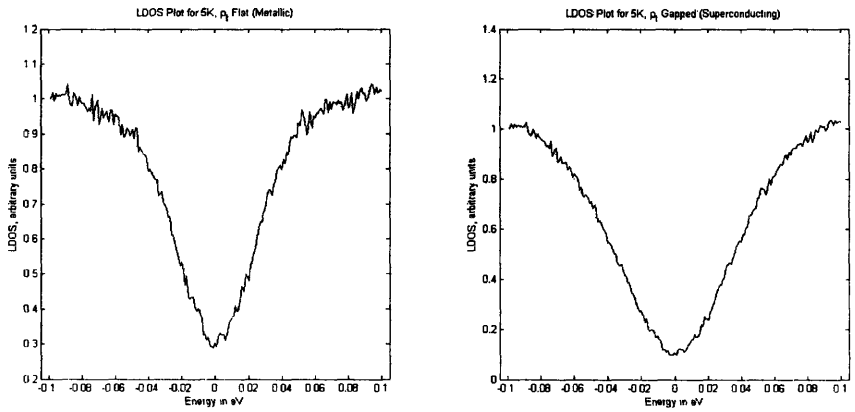


Figure 3.3: The right is the inferred LDOS if both sample and tip have triangular gaps. The resulting gap is roughly twice as wide as the gaps on the sample and tip (left).

Note that the gap is twice the width of the gap in either the sample or tip. It appears from this, along with other similar simulations, that the inferred LDOS plot is a convolution of $\rho_s$ and $\rho_t$. If a superconducting tip is used in measurements (or if a large portion of the sample is accidentally picked up by the tip), it may still be possible to gain information about the sample LDOS via deconvolution (assuming the tip LDOS is known) or by dividing measured gaps by 2 (if some of the sample has been picked up and is being used as a tip).

## 3.4 Tip Height Noise

Vibrational noise often limits topography resolution in STM studies. Here, we will look at how noise in tip height affects spectroscopy. Though all of the tip noise in our simulation is white (up to the 10 kHz simulation frequency), it is shaped by filters along the way, both linear (preamp, lock-in) and nonlinear (quantum mechanics of tip tunneling).

Figure 3.4 shows how different amounts of tip noise (expressed as a fraction of the tunneling constant $s_0 = 1$ Å) affect the measured spectrum.

## 3.5 Changes in the Applied Sample Voltage

Recall that voltage applied to the sample corresponds of a DC componenet (or bias) with an AC signal added to probe how the LDOS changes around the bias voltage. The default settings use a DC step size of 1 mV, starting at -100 mV, and an AC amplitude of 2.5 mV. Figure 3.5 shows the effect of increasing the DC step size and decreasing the AC amplitude.

## 3.6 Current Preamplifier Noise

We typically observe tunneling currents around 50 pA with noise levels of about 5 pA, or 10%. Here we investigate the sensitivity of the measured signal to noise in

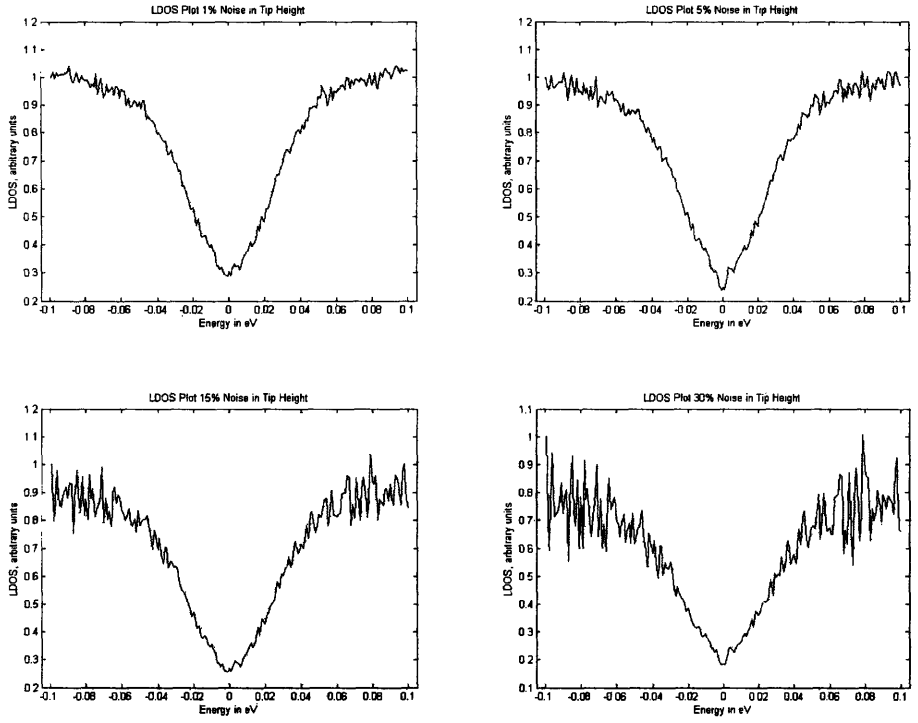


Figure 3.4: Effect of tip height noise on measured LDOS. Noise of 15% corresponds to an integrated spectral density (total power) of 15% of the tunneling constant $s_0$. The power spectrum is white (flat) up to 10 kHz.

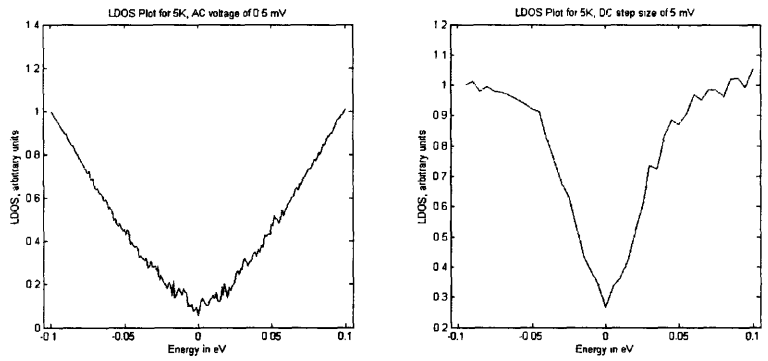


Figure 3.5: The left plot shows the effect of decreasing the AC signal to 0.5 mV (20% of its default value). This is not large enough to compensate for the tip and current noise, resulting in an inaccurate LDOS plot. For the right plot, we have increased the DC step size from 1 mV to 5 mV. While this looks choppier than other plots, it captures all of the important features.

the preamp. The actual amount of noise generated by the preamplifier is limited thermal restrictions (Johnson Noise).

Figure 3.6 shows that the resulting measurement is quite robust to large amounts of white noise introduced by the preamplifier. This is partially due to the averaging that takes place in the ECU.

## 3.7 Averaging Time

Varying the computer averaging time has a very small effect on the outputted LDOS (see Figure 3.7). It is likely that the necessary averaging is being carried out by the low-pass filters in the preamp and lock-in. This suggests that it may be wise to step rapidly and spend less time averaging with the computer.

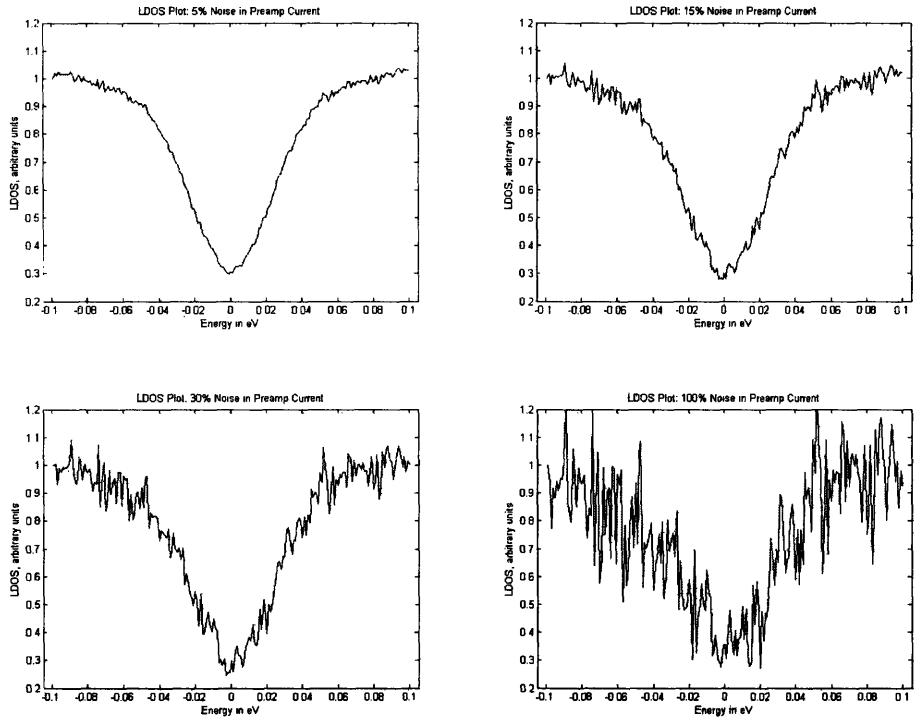


Figure 3.6: Plots of LDOS for various amounts of current preamplifier noise. The gap can be resolved even when the noise is comparable to the rms value of the current (Remember, some averaging takes place in the ECU to help reduce noise)

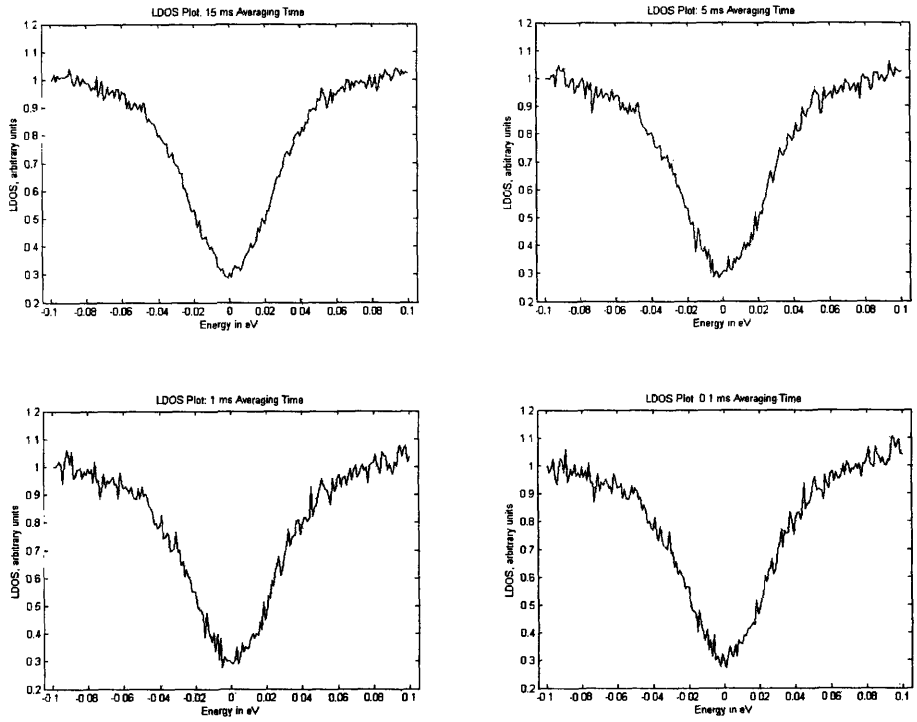


Figure 3.7: Plots of LDOS for various ECU averaging times. The sensitivity of the output to averaging time is negligible.

# Appendix: Using the Simulation Software

The simulation software consists of three separate files. The simulation of the tip and the electronics are both Simulink® programs (`simulation.mdl` and `lockin.mdl`) while the averaging done by the ECU is handled my a separate (simple) function defined in `ecuaverage.m`.

In `simulation.mdl` you can change the temperature, $\rho_s$, $\rho_t$, or how the integrated tunneling current is obtained. This program will output two files, `voltage.mat` and `current.mat`. The former contains the voltage supplied to the sample and will be needed by the `ecuaverage.m` later. The latter contains the integrated current obtained from the sample, normalized to have an rms value of 1.

The lock-in amplifier and preamplifier are handled in `lockin.mdl`. Here you can change parameters such as the filters being used (different settings on the lock-in and preamplifier correspond to different linear filters). Also adjustable here are the preamplifier noise and lock-in frequency (though this should match the signal used to bias the sample, which it references in real life).

Finally, use `ecuaverage` on the output of `lockin.mdl` along with `voltage.mat` to obtain LDOS($E$). The usage for this is `ecuaverage(voltage,lockin,P,T)`, where `P` is the length of time between DC steps and `T` is the desired averaging time.

# Bibliography


[1] J. Bardeen, L. N. Cooper, and J. R. Schrieffer, *Theory of Superconductivity*, Physical Review **108** (1957), 1175–1204.

[2] G. Binnig, H. Rohrer, C. Gerber, and E. Weibel, *Surface Studies by Scanning Tunneling Microscopy.*, Physical Review Letters **49** (1982), 57–61.

[3] J. Hoffman, *Search for Alternative Electronic Order in the High Temperature Superconductor $Bi_2Sr_2CaCu_2O_{8+\delta}$ by Scanning Tunneling Microscopy.*, Ph.D. Thesis, University of California, Berkeley (2003).

[4] DL Instruments, *Applying the Model 1211 Current Preamplifier to Tunneling Microscopy*, IAN **55** (1987).